



# Estimating Surface Runoff Potential in the Abyan Delta, Yemen Using GIS-Based SCS-Curve Number Method

Marwan Al-Badani<sup>1,2 \*</sup>, Zamzam Mubarak<sup>2</sup> and Sady Alsady<sup>2,3</sup>

<sup>1</sup>Department of Geology and Environment, Faculty of Applied Science, Dhamar University, Dhamar, Yemen,

<sup>2</sup>Water and Environment Center, Sana'a University, Sana'a, Yemen,

<sup>3</sup>UNICEF Organization, Yemen.

\*Corresponding author: [mrwan87@yahoo.com](mailto:mrwan87@yahoo.com)

## ABSTRACT

A GIS-based Soil Conservation Service Curve Number (SCS-CN) approach was used to estimate surface-runoff potential in Yemen's arid Abyan Delta ( $\sim 1,237 \text{ km}^2$ ). Sentinel-2 (10 m) imagery was classified into major land-cover types and combined with hydrologic soil groups (HYSOGs) to assign CN values under Antecedent Moisture Condition II. The composite CN map (67–100; mean = 91.8) indicates limited infiltration across large areas of bare or impervious surfaces on clayey soils. Using the standard SCS-CN equations, event runoff was simulated for representative storm depths of 74, 124, and 174 mm. The model produced direct-runoff depths of  $\sim 52$ , 100, and 150 mm, corresponding to runoff coefficients of  $\sim 71\%$ , 81%, and 86%, and basin-wide volumes of 0.65, 1.24, and  $1.85 \times 10^8 \text{ m}^3$ , respectively. Spatial attribution shows that high-CN zones (notably barren HSG-C/D units and built-up/roads) generate most of the runoff despite covering a smaller fraction of the delta. The results identify priority areas for spate-irrigation, retention, and recharge interventions, and provide a reproducible baseline for flood-risk reduction and water-harvesting planning in data-scarce drylands. The workflow can be readily updated with improved soils, land-use, or climate inputs to support adaptive management.

## ARTICLE INFO

### Keywords:

Surface runoff, Curve Number, GIS, Remote sensing, Arid hydrology, Abyan Delta.

### Article History:

Received: 29-June-2025,

Revised: 21-July-2025,

Accepted: 1-August-2025,

Available online: 28 October 2025.

## 1. INTRODUCTION

Efficient capture of floodwater is critical in arid regions such as the Abyan Delta in southern Yemen, where agriculture depends on episodic spate flows and declining groundwater reserves. Previous studies have documented the delta's hyper-arid climate and limited rainfall [1, 2]. For example, Ewea (2007) reported that mean annual precipitation on the coastal plain is only 50–100 mm, rarely exceeding 100 mm in the delta, while higher rainfall ( $>200 \text{ mm}$ ) occurs only in the adjacent highlands. Most effective rainfall comes during short monsoon storms (July–September), yet potential evapotranspiration exceeds  $2,000 \text{ mm yr}^{-1}$ , resulting in severe water scarcity. With a population of  $\sim 20,000$  in Zinjibar town heavily reliant on irrigation, understanding runoff

generation is vital for water harvesting, spate irrigation, and recharge planning.

The Soil Conservation Service Curve Number (SCS-CN) method, developed by the USDA, is one of the most widely used empirical models for estimating direct runoff from rainfall. It integrates precipitation, land cover, soil type, and moisture conditions into a simple equation that requires relatively limited data [3, 4]. Recent studies have demonstrated the benefits of combining SCS-CN with GIS and remote sensing, which enable spatially explicit runoff estimates in data-scarce basins. Applications include catchments in Palestine [5], India [6], and Saudi Arabia [7], all showing reliable performance. Similar approaches have been applied globally to arid basins for flood assessment and water-resource planning [8–10].

Despite these advances, few studies have investi-

gated runoff in southern Yemen, where data limitations are acute. No gauge records exist in the Abyan Delta to calibrate rainfall–runoff models, making physically based estimates essential. The delta's combination of sparse vegetation, clay-rich soils, and intense storms creates conditions highly favorable to runoff generation, yet quantitative assessments remain scarce.

This study applies a GIS-based SCS-CN method to the Abyan Delta to provide the first systematic spatial analysis of runoff potential in the basin. The specific objectives are to: (i) generate an up-to-date land use/land cover (LULC) map, (ii) assign curve numbers to produce a composite CN map under normal antecedent moisture conditions (AMC II), and (iii) compute runoff depths and volumes for representative storm events. The results aim to identify runoff-prone areas, quantify potential runoff volumes, and provide a baseline for floodwater harvesting, recharge, and risk management in this arid and data-scarce region.

## 2. MATERIALS AND METHODS

### 2.1. STUDY AREA

The study focuses on the Abyan Delta in southern Yemen, a coastal alluvial plain where Wadi Bana and Wadi Hassan terminate and deposit floodwaters. Geographically, the delta lies between latitudes 12°39'N–13°08'N and longitudes 44°40'E–45°06'E, covering an area of  $\sim 1,237 \text{ km}^2$  (Figure 1). It forms part of the larger Abyan–Tuban sedimentary basin and is drained mainly by the seasonal channels of Wadi Tuban and Wadi Bana.

The climate is hyper-arid, with mean annual rainfall on the delta floor of  $\sim 50$ –100 mm [1]. Rainfall increases inland, reaching  $\sim 370 \text{ mm yr}^{-1}$  on Wadi Bana and  $\sim 250 \text{ mm yr}^{-1}$  on Wadi Hassan. Precipitation occurs mainly in short, intense monsoon storms (July–September), while potential evapotranspiration exceeds 2,000 mm  $\text{yr}^{-1}$ , resulting in severe water deficits. Agriculture is predominantly spate-irrigated, and  $\sim 70\%$  of Zinjibar's residents depend on farming. Groundwater abstraction is high ( $70$ – $100 \times 10^6 \text{ m}^3 \text{ yr}^{-1}$ ), leading to declining aquifer levels. These conditions make the capture and management of floodwater essential for sustaining irrigation and recharge.

### 2.2. DATA SOURCES

A range of spatial datasets was assembled (Table 1). Sentinel-2 multispectral imagery (10 m, 2024) from the Yemeni Remote Sensing Center was used for land-cover mapping. A 12.5 m DEM was used to delineate catchments and topography. Geological data were derived from the 1:250,000 national map [12]. Hydrologic soil groups (HSGs) were obtained from the global HYSGOs250m dataset [13]. Long-term rainfall patterns were characterized using CRU TS v4.0 gridded data

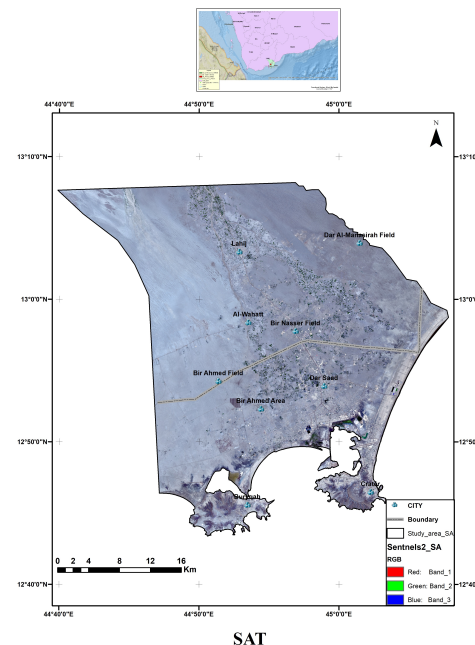


Figure 1. Satellite image of the study area (Sentinel-2, [11])

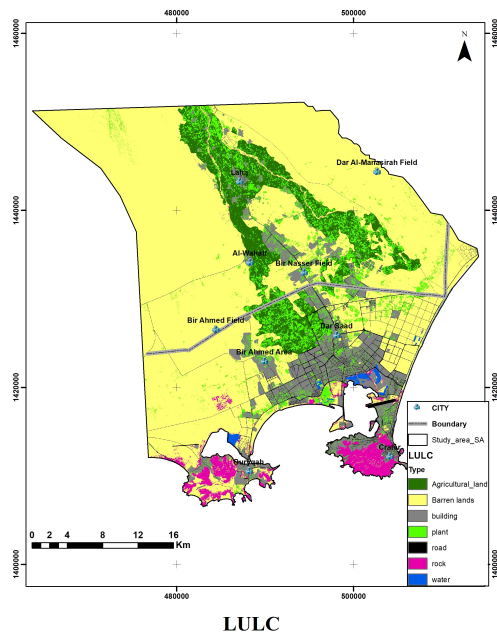
(2011–2020). All layers were projected to WGS84 UTM Zone 38N and resampled to 10 m.

Table 1. Primary datasets used in the study.

Data Type	Scale / Resolution	Year	Source	Usage
Sentinel-2 Imagery	10 m	2024	[11]	Land use/cover classification
DEM	12.5 m	2024	[11]	Terrain delineation
Geological Map	1:250,000	1990	[12]	Lithology / hydrogeology
Hydrologic Soil Groups	250 m	2018	[13]	Soil infiltration classes
Rainfall Data	0.5°	2011–2020	[14]	Precipitation climatology

### 2.3. LAND USE AND LAND COVER (LULC)

An LULC map (Figure 2) was produced using supervised classification of Sentinel-2 imagery. Training samples were drawn from known land-cover sites and classified with a Maximum Likelihood algorithm. Major classes include: urban/built-up (settlements, roads), agricultural fields, barren land, natural vegetation, and wadi channels. Misclassifications were corrected through visual inspection, ensuring  $\sim 85\%$  accuracy.



**Figure 2.** Land Use/Land Cover (LULC) map of the study area.

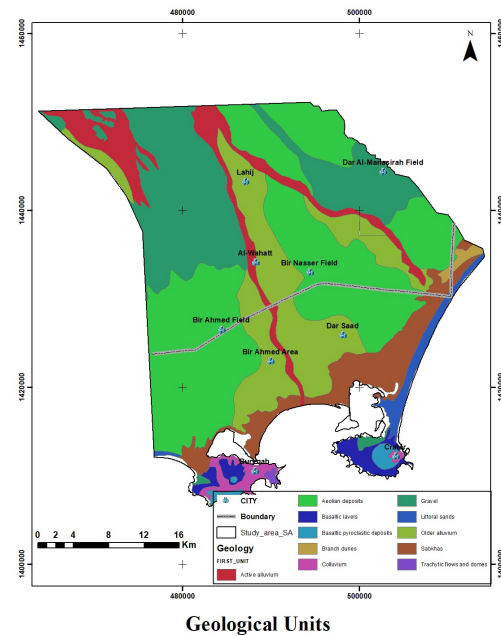


**Figure 3.** Geological map of the Abyan Delta [12].

#### 2.4. GEOLOGICAL AND SOIL DATA

The delta is underlain by alluvial and deltaic deposits, with limited bedrock exposures at the margins (Figure 3). While not directly used in CN assignment, geology provides important context for infiltration capacity.

Soil infiltration properties were mapped using the HYSOGs dataset. Soils were classified into SCS hydrologic groups A–D, ranging from high infiltration (A) to very low (D). Much of the delta comprises HSG B and C, with low-lying clayey areas in HSG D (Figure 4).

#### 2.5. RAINFALL DATA

Rainfall was mapped using CRU gridded data to show long-term spatial variability (Figure 5). Mean annual rainfall ranges from  $\sim 74$  mm in the western delta to  $\sim 174$  mm near the eastern uplands. For runoff simulations, three representative rainfall depths (74, 124, 174 mm) were selected to represent low, medium, and high events.

#### 2.6. CURVE NUMBER ASSIGNMENT AND RUNOFF ESTIMATION

The SCS-CN method was implemented in GIS. Each LULC–HSG combination was assigned a CN value under AMC II using USDA-NRCS [3], [15] lookup tables (e.g., irrigated cropland on clay = CN 91; natural vegetation on sandy soils = CN 77; bare clay = CN 91; paved/impervious = CN 98). Overlaying the LULC and

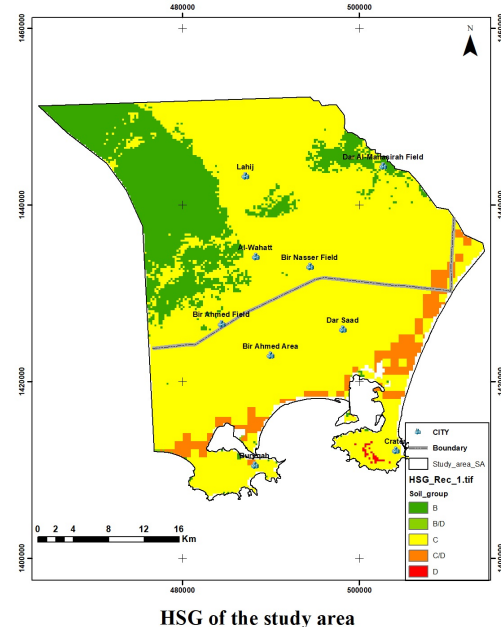
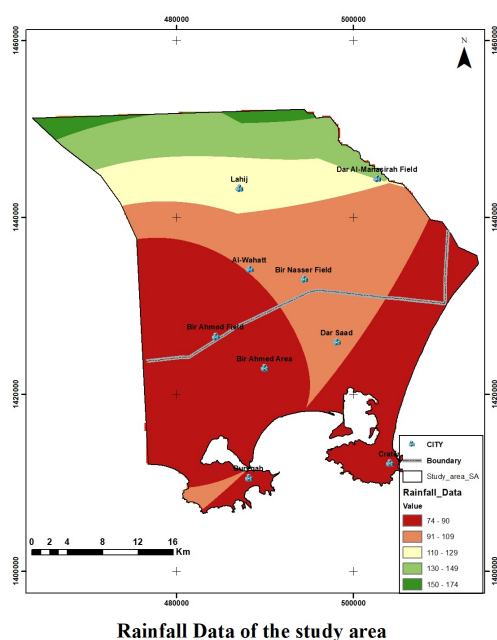


**Figure 4.** Hydrologic Soil Group (HSG) distribution [13].

HSG layers produced a composite CN map at 10 m resolution (Figure 6).

Runoff depths were simulated for rainfall events of 74, 124, and 174 mm using the standard SCS-CN equations



Rainfall Data of the study area

**Figure 5.** Mean annual rainfall distribution across the Abyan Delta [14].

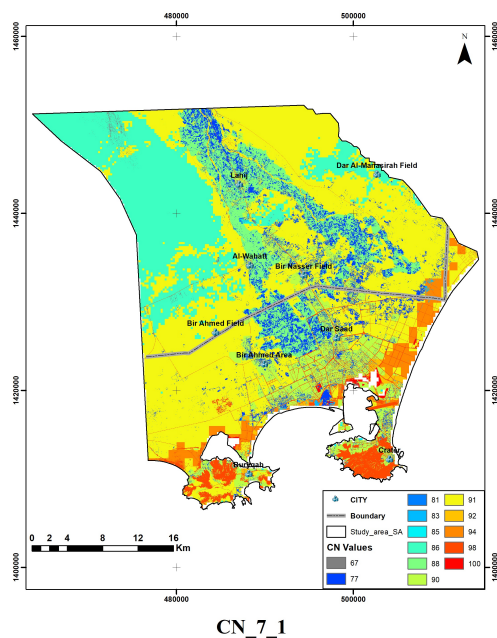


**Figure 6.** Curve Number (CN) map under AMC II conditions.

[15]:

$$S = \frac{25400}{CN} - 254, \quad I_a = 0.2S,$$

$$Q = \begin{cases} 0, & P \leq I_a \\ \frac{(P-I_a)^2}{P-I_a+S}, & P > I_a \end{cases}$$

where  $S$  is potential maximum retention (mm),  $I_a$  is initial abstraction,  $P$  is rainfall (mm) and  $Q$  is runoff depth (mm). The model was run at cell scale and aggregated for basin-wide runoff volumes ( $Q \times \text{area}$ ). All processing was performed in GIS using raster algebra.

## 3. RESULTS

### 3.1. CURVE NUMBER MAP

The composite Curve Number (CN) map (Figure 6) was generated by intersecting LULC and HSG layers under AMC II conditions. CN values across the delta range from 67 to 100, reflecting strong spatial contrasts in soil–land cover complexes. Low values ( $\sim 67$ –77) occur where permeable soils (HSG B) coincide with natural vegetation, indicating higher infiltration and limited runoff. In contrast, CN values approaching 100 characterize open water and impervious urban surfaces with negligible infiltration.

The area-weighted mean CN for the basin is 91.8, signifying a dominant landscape of low to moderate infiltration potential. This high composite CN highlights the delta's strong propensity for generating runoff, with limited rainfall retained before surface flow commences. Most of the area lies within the 80–95 CN range, consistent with sparse vegetation and clayey soils.

Table 2 summarizes the spatial distribution of LULC–HSG combinations. Barren land on HSG C (CN = 91) is the single largest category, covering  $\sim 44.7\%$  of the delta. Barren land on HSG B (CN = 86) accounts for 20.1%. Agriculture on HSG C (CN = 88) occupies  $\sim 9.2\%$ , while natural vegetation on HSG C (CN = 77) makes up  $\sim 8\%$ . Built-up areas and roads (CN 90–98), together with rocky outcrops, comprise  $\sim 13\%$  of the surface, acting as near-immediate runoff sources. Open water bodies (CN = 100) cover  $< 1\%$  but represent zones of zero retention. These distributions confirm that most of the delta is dominated by surfaces with high runoff potential (Figure 7).

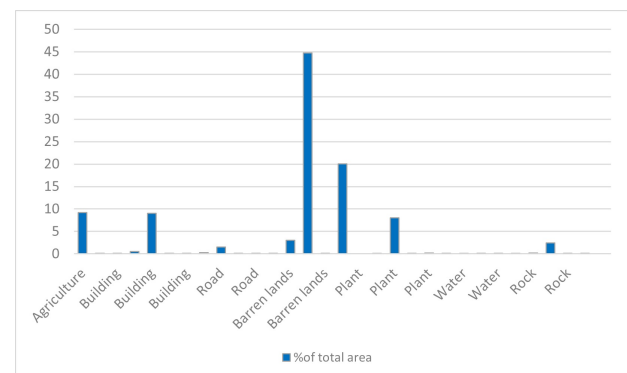


**Figure 7.** Areal distribution of LULC–HSG classes and CN values.

**Table 2.** Area and percentage distribution of LULC–HSG combinations with assigned Curve Numbers (CN) under AMC II conditions.

LULC Group	HSG	CN	Area (km <sup>2</sup> )	% of Total
<b>Agriculture</b>	C	88	113.39	9.165
<b>Agriculture</b>	B	81	0.18	0.014
<b>Building</b>	D	92	0.06	0.005
<b>Building</b>	C/D	92	6.22	0.502
<b>Building</b>	C	90	112.31	9.078
<b>Building</b>	B/D	92	0.02	0.002
<b>Building</b>	B	85	0.95	0.077
<b>Road</b>	C/D	98	3.80	0.307
<b>Road</b>	C	98	19.45	1.572
<b>Road</b>	B/D	98	0.01	0.001
<b>Road</b>	B	98	0.31	0.025
<b>Barren lands</b>	D	94	0.11	0.009
<b>Barren lands</b>	C/D	94	37.59	3.038
<b>Barren lands</b>	C	91	553.12	44.707
<b>Barren lands</b>	B/D	94	0.24	0.019
<b>Barren lands</b>	B	86	248.53	20.088
<b>Plant</b>	D	83	0.00	0.000
<b>Plant</b>	C/D	83	1.90	0.153
<b>Plant</b>	C	77	98.99	8.001
<b>Plant</b>	B/D	83	0.01	0.001
<b>Plant</b>	B	67	2.27	0.184
<b>Water</b>	C/D	100	0.84	0.068
<b>Water</b>	C	100	1.75	0.141
<b>Water</b>	B/D	100	0.16	0.013
<b>Water</b>	B	100	0.25	0.020
<b>Rock</b>	D	98	1.39	0.112
<b>Rock</b>	C/D	98	2.64	0.213
<b>Rock</b>	C	98	30.13	2.436
<b>Rock</b>	B/D	98	0.10	0.008
<b>Rock</b>	B	98	0.50	0.040

### 3.2. RETENTION AND INITIAL ABSTRACTION

Using the composite CN of 91.8, the potential maximum retention was calculated as:

$$s = \frac{25400}{91.8} - 254 \approx 22.7 \text{ mm}$$

The initial abstraction was estimated as  $I_a = 0.2s \approx 4.5 \text{ mm}$ . This implies that, on average, the first 4-5 mm of rainfall is lost to interception and infiltration. Once cumulative rainfall exceeds  $\sim 23 \text{ mm}$ , soils are effectively saturated and subsequent rainfall contributes directly to runoff.

### 3.3. RAINFALL–RUNOFF SIMULATION

Runoff depths (Q) were estimated for storm events of 74, 124, and 174 mm (Table 3). Even moderate storms yielded high runoff fractions.

For  $P = 74 \text{ mm}$ , runoff depth was  $\sim 52 \text{ mm}$ , representing  $\sim 71\%$  of rainfall. For  $P = 124 \text{ mm}$ ,  $\sim 100 \text{ mm}$  (81%) became runoff, while for the extreme event of 174 mm,  $\sim 150 \text{ mm}$  (86%) ran off. These results illustrate

**Table 3.** Runoff depths for representative rainfall events (AMC II, CN = 91.8).

Rainfall P (mm)	P – I <sub>a</sub> (mm)	Runoff Q (mm)	% of Rainfall
74	69.5	52.4	70.8%
124	119.5	100.4	81.0%
174	169.5	149.5	85.9%

the strongly nonlinear rainfall–runoff relationship (Figure 8). As rainfall increases, both absolute runoff and runoff coefficients rise rapidly because soil storage (S) is fixed; once exceeded, nearly all additional rainfall becomes surface flow.

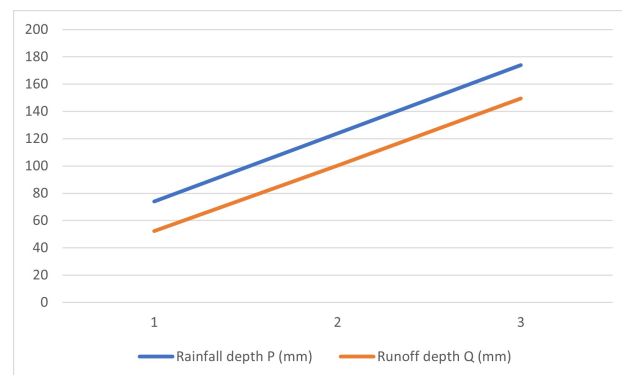


**Figure 8.** Rainfall–runoff curve for the Abyan Delta (AMC II, CN = 91.8).

### 3.4. RUNOFF VOLUMES

Runoff depths were converted into basin-wide runoff volumes using the total area of 1,237 km<sup>2</sup> (Table 4).

**Table 4.** Runoff depth and volume estimates for selected storm events.

Rainfall (mm)	Runoff depth (mm)	Runoff volume (10 <sup>8</sup> m <sup>3</sup> )
74	52.4	0.65
124	100.4	1.24
174	149.5	1.85

A moderate storm of 124 mm produces  $\sim 1.24 \times 10^8 \text{ m}^3$  of runoff across the delta, equivalent to more than 100 million cubic meters of water. Even smaller events (74 mm) generate  $\sim 65$  million cubic meters, while extreme events exceed 180 million cubic meters. These volumes underline both the substantial flood risk and the opportunity to harvest and store runoff.

### 3.5. KEY INSIGHTS

- Dominant runoff sources:** Barren clayey soils (CN 86–91) and built-up/road surfaces generate most of the runoff, though they cover only  $\sim 58\%$  of the area.

- **Limited retention:** With  $S \approx 22.7$  mm, only a small fraction of rainfall is absorbed before saturation.
- **High runoff coefficients:** Even moderate storms yield  $> 70\%$  runoff, consistent with conditions in arid, sparsely vegetated basins.
- **Management potential:** Capturing a portion of the  $1.24 \times 10^8$  m<sup>3</sup> from a single median storm could significantly augment water supply for irrigation and groundwater recharge.

## 4. DISCUSSION

### 4.1. RUNOFF CHARACTERISTICS IN THE ABYAN DELTA

The results indicate that the Abyan Delta has an exceptionally high runoff potential under typical arid conditions. With a composite CN of  $\sim 91.8$ , the basin retains only  $\sim 2$  mm of rainfall before producing surface flow. Simulated runoff coefficients of 71–86% are consistent with the very limited infiltration capacity of the clay-rich, sparsely vegetated landscape. The rainfall–runoff curve showed a near-linear response ( $R^2 \approx 0.98$ ) across the tested storm depths, confirming that once initial retention is exceeded, additional rainfall translates almost directly to runoff.

### 4.2. COMPARISON WITH OTHER STUDIES

These findings align with results from other arid and semi-arid basins. [16] achieved similar  $R^2$  values in Saudi Arabia, while [17] reported average runoff  $\sim 76\%$  in a Yemeni wadi, close to the 80–86% observed here for larger storms. [18] validated SCS-CN estimates in Egypt within 5–12% of measured flood volumes, confirming the method's reliability. Comparable studies in Palestine [5] and Ethiopia [19] also observed rising runoff coefficients with increasing storm size, a trend replicated in the Abyan Delta. Overall, the estimated CN ( $\sim 92$ ) and runoff fractions fall at the higher end of global reports, reflecting the dominance of clay-rich soils.

### 4.3. WATER RESOURCE IMPLICATIONS

The modeled runoff volumes are substantial. A single 124 mm storm could generate  $\sim 1.24 \times 10^8$  m<sup>3</sup>, sufficient to irrigate 1,000–2,000 ha at typical application depths. Even smaller events yield tens of millions of cubic meters, underscoring opportunities for spate irrigation, retention basins, and recharge structures. Prioritizing barren clay-rich areas and built-up zones for water-harvesting interventions would maximize benefits while reducing flood hazards. These results also support proposals for infiltration galleries and check dams in the delta plain to replenish shallow aquifers.

### 4.4. MODEL LIMITATIONS

Despite its utility, the SCS-CN method has limitations. It assumes uniform rainfall and fixed antecedent conditions, omits slope and storm-duration effects, and neglects channel routing or surface roughness. In steep tributaries, slope-adjusted CN values may be required [20]. The analysis also relied on secondary datasets: HYSGOs soils at 250 m and LULC classification with  $\sim 85\%$  accuracy. Furthermore, no flow gauges exist in the delta to calibrate or validate runoff predictions, so results should be considered first-order estimates.

### 4.5. FUTURE RESEARCH

Improvements could include:

- **Sensitivity to antecedent moisture:** Modeling AMC I (dry) and AMC III (wet) conditions, which may shift composite CN from  $\sim 83$  to  $\sim 96$ .
- **Climate variability:** Testing multi-year drought and wet periods, or incorporating downscaled climate-change projections.
- **Hydrodynamic routing:** Coupling SCS-CN outputs with HEC-HMS or HEC-RAS to predict flood-wave timing, discharge peaks, and inundation.
- **Field calibration:** Installing monitoring stations to capture high-water marks or hydrographs during storm events for refining CN values.

Such extensions would enhance predictive accuracy and support climate-resilient water management.

### 4.6. PRACTICAL IMPLICATIONS

The study highlights actionable priorities for the Abyan Delta:

- **Flood risk mitigation:** High-CN zones such as urbanized areas, rocky outcrops, and clay-rich barren fields should be targeted for levees, diversion structures, and early warning systems.
- **Rainwater harvesting:** Capturing even a fraction of runoff from a typical storm could substantially increase water availability for irrigation and aquifer recharge.
- **Scalable planning:** The GIS-based SCS-CN framework is cost-effective, relies mainly on remote sensing and global datasets, and can be easily updated as better inputs become available. This makes it adaptable for use in other Yemeni watersheds where hydrological data are scarce.

## 5. CONCLUSION

The hyper-arid Abyan Delta exhibits one of the highest runoff potentials observed in semi-arid to arid basins, driven by clay-rich soils, sparse vegetation, and episodic



storm events. The GIS-based SCS-CN analysis produced a composite CN of 91.8 under AMC II, corresponding to a maximum retention of  $\sim 22.7$  mm and an initial abstraction of  $\sim 4.5$  mm. Simulations for rainfall depths of 74–174 mm generated runoff coefficients of 71–86% and volumes of  $6.5 \times 10^7$ – $1.85 \times 10^8$  m<sup>3</sup> across the 1,237 km<sup>2</sup> delta. Although barren and impervious areas cover less than half of the surface, they account for  $\sim 57\%$  of runoff, making them critical targets for water-harvesting and flood-mitigation measures.

These findings emphasize the potential for spate irrigation, retention basins, and infiltration galleries to redirect stormflow, reduce downstream flood risks, and replenish overexploited aquifers. The methodology is cost-effective, relying on freely available satellite imagery, global soil datasets, and GIS tools, and can be updated as new data emerge. Applying this framework more widely across Yemen's ungauged basins could establish a regional basis for runoff assessment and resource planning.

Future research should test the model under varying antecedent moisture conditions, integrate hydrodynamic routing tools to capture flood-wave dynamics, validate outputs with field measurements, and assess climate and land-use change scenarios. Advancing these efforts will refine predictive capacity and support adaptive management. Ultimately, harnessing the delta's episodic floods offers a pathway toward improved water security, agricultural resilience, and socio-economic stability in Yemen and similar arid regions.

#### Ethics Statement

This study used publicly available satellite imagery and secondary geospatial datasets and did not involve human or animal subjects or identifiable personal data. Ethics approval: Not applicable.

#### CRediT Author Contributions

Conceptualization: Marwan Al-Badani

Methodology: Marwan Al-Badani, Zamzam Mubarak

Data curation: Zamzam Mubarak

Formal analysis: Marwan Al-Badani

Investigation (field/context): Marwan Al-Badani, Sady Alsady

Resources: Water & Environment Center (WEC), UNICEF Yemen

Software (GIS/remote sensing): Marwan Al-Badani

Visualization: Marwan Al-Badani

Writing – original draft: Marwan Al-Badani

Writing – review & editing: Zamzam Mubarak, Sady Alsady

#### Conflict of Interest

The authors declare no conflicts of interest regarding the publication of this study. All coauthors have approved

the manuscript and concur with its submission to the journal.

#### Funding Statement

This study funding by IHE Delft, SFD Yemen, and WEC Sana'a University **URaHa Scholarship**.

## REFERENCES

- [1] H. Ewea, "Assessment of potential water resources in abyans area – southern yemen," *Civ. Eng. Res. Mag.* **23**, 785–795 (2007).
- [2] K. Atroosh and A. Moustafa, "An estimation of the probability distribution of wadi bana flow in the abyans delta of yemen," *J. Agric. Sci.* **4**, 80 (2012).
- [3] USDA Soil Conservation Service, *National Engineering Handbook, Section 4: Hydrology* (U.S. Government Printing Office, Washington, D.C., 1985).
- [4] S. Mishra and V. Singh, "Another look at the scs cn method," *J. Hydrol. Eng.* **4**, 257–264 (1999).
- [5] M. Shadeed and M. Almasri, "Application of gis based scs cn method in west bank catchments, palestine," *Water Sci. Eng.* **3**, 1–14 (2010).
- [6] A. Ranjan, H. Mishra, V. Yadav, and S. Singh, "Estimation of runoff using curve number method for the kaushambi microwatershed, allahabad region, india," *J. Pharmacogn. Phytochem.* **9**, 208–214 (2020).
- [7] H. Al-Ghabari and A. Dewidar, "Integrating gis based mcda techniques and the scs cn method for identifying potential zones for rainwater harvesting in a semi-arid area," *Water* **13**, 704 (2021).
- [8] T. Gitika and S. Ranjan, "Estimation of surface runoff using nrccs curve number procedure in buriganga watershed, assam, india – a geospatial approach," *Int. Res. J. Earth Sci.* **2**, 1–7 (2014).
- [9] M. Al Saud, "Morphometric analysis of wadi aurnah drainage system, western arabian peninsula," *Open Hydrol. J.* **3**, 1–10 (2009).
- [10] G. Dawod, M. Mirza, and K. Al Ghadri, "Gis based estimation of flood hazard impacts on road network in makkah city, saudi arabia," *Environ. Earth Sci.* **67**, 2205–2215 (2012).
- [11] Yemeni Remote Sensing Center, "Sentinel-2 multispectral satellite imagery (10 m)," (2024).
- [12] Yemen Geological Survey & Mineral Resources Board, *Geological Map of Yemen (1:250,000), 2nd edn* (Ministry of Oil & Minerals, Sana'a, 1990).
- [13] A. Ross, Y. Wei, R. Hall, and T. Ault, "Hysogs250m: Global gridded hydrologic soil groups for curve number based runoff modeling," *Sci. Data* **5**, 180091 (2018).
- [14] I. Harris, T. Osborn, P. Jones, and D. Lister, "Version 4 of the cruts high resolution gridded climate dataset," *Sci. Data* **7**, 109 (2020).
- [15] NRCS, *Estimating Direct Runoff from Storm Rainfall* (USDA NRCS, 2004).
- [16] H. Al-Ghabari, A. Dewidar, and A. Alataway, "Estimation of surface water runoff for a semi-arid area using rs and gis based scs cn method," *Water* **12**, 1924 (2020).
- [17] T. Taher, "Integration of gis database and scs-cn method to estimate runoff volume of wadis of intermittent flow," *Arab. J. for Sci. Eng.* **40**, 685–692 (2015).
- [18] M. Khattab, M. Fadl, H. Megahed *et al.*, "Evaluation of scs cn for flash flood runoff estimation in arid regions: a case study of the central eastern desert, egypt," *Hydrology* **12**, 54 (2025).
- [19] A. Mulu, S. Kassa, R. Abiye *et al.*, "Runoff estimation using the scs cn method and gis: a case study in the wuseta watershed, upper blue nile, ethiopia," *Discov. Water* **5**, 32 (2025).
- [20] I. Peker, S. Gülbaz, V. Demir, *et al.*, "Integration of hec ras and hec hms with gis in flood modeling and flood hazard mapping," *Sustainability* **16**, 1226 (2024).